

Generalized LUI propagation model for UAVs communications using terrestrial cellular networks

Tiago Tavares^{1,2}, Pedro Sebastião^{1,2}, Nuno Souto^{1,2},
Francisco Cercas^{1,2}, Marco Ribeiro^{1,2} and Américo
Correia^{1,2}

Instituto de Telecomunicações, ISCTE – IUL
Av. das Forças Armadas
1649-026 Lisboa, Portugal
tiagofltavares@gmail.com; {pedro.sebastiao, nuno.souto,
francisco.cercas, marco.ribeiro, americo.correia}@iscte.pt

Fernando J. Velez¹
Instituto das Telecomunicações - DEM
Universidade da Beira Interior
Faculdade de Engenharia
6200-026 Covilhã, Portugal
fjv@ubi.pt

Abstract—This work proposes an empirical propagation model to obtain the path loss, and therefore determine the average received power, of a signal for a specific outdoor urban scenario with UAVs. The proposed 3D propagation model for terrestrial cellular networks generalizes the LUI model and is valid in the frequency ranges from GSM, UMTS and LTE technologies. We report experimental work in 3D space, considering the height, the antennas base station tilt, sectorization, angle and distances profile. The experimental work included in this study appropriately agrees with the proposed theoretical model; hence, the proposed model is adequate for cellular planning tools.

Keywords— Propagation model, GSM, UMTS, LTE, hexacopter, UAV, 3D propagation model

I. INTRODUCTION

The development of the propagation model proposed in this paper is part of the SAAS (Remote Piloted Semi-Autonomous Aerial Surveillance System Using Terrestrial Wireless Networks) project from Instituto de Telecomunicações, which involves considering an Unmanned Aerial Vehicles (UAVs) and the existing mobile cellular networks to transmit real-time video and other telemetry data while simultaneously receiving control commands during flight. UAVs have been around for many years. However, with the advance in technology new types of UAVs started to appear facilitating to accomplish different tasks that were not previously possible to execute before. The hexacopter is an example of this innovation. It can be used to perform several tasks that would be harder for a person to do.

To reliably communicate between the terrestrial transmitter antenna and the hexacopter antenna the received power has to exceed the receiver sensitivity. Hence, it is worthwhile to analyze the signal propagation conditions, which justifies the development of a propagation model for the type of scenario with similar air interface conditions. The model being developed, like many others, depends on several parameters, for example, frequency range, distance, base station height and tilt angles, antenna pattern, obstacles, etc.

To assess this propagation model, the first step has been to study the several propagation models available in the literature

as well as the mobile technologies that are going to be considered in the propagation model. The approach to assess the empirical model has consisted of performing measurements in real environments while comparing them with simulated and theoretical results.

Most of the existing propagation models for outdoor environments are developed considering the path between the terrestrial terminal station and the base station (path #1), as shown in Fig. 1. However, the model proposed in this work also addresses the behaviour of the propagation channel over the path between the base station and the UAV terminal station (path #2). Adequate propagation conditions facilitate high quality data transfer and video communications.

Another objective of the underlying research is to know the channel behaviour when the hexacopter enters the area above the base station. By knowing the received power or path loss, the model allows estimating if the connection is going to be lost, and possibly trigger handover if the terminal station antenna still receives enough power from another base station antenna located nearby, on the top of a higher building.

The development of the proposed empirical model is based on an analysis of existing propagation models and its verification results from field trials.

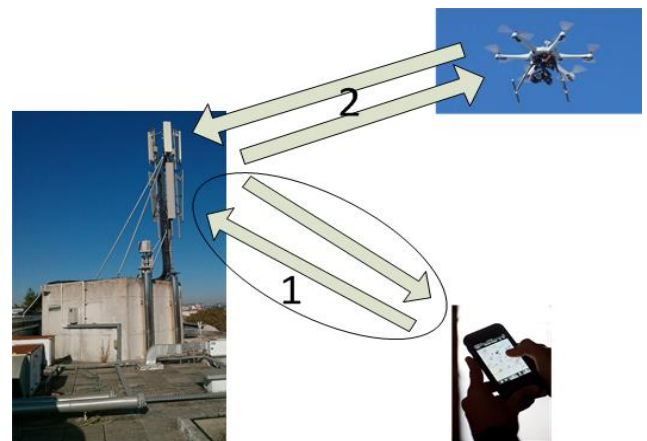


Fig. 1. – Identification of the propagation channel paths between the base station and terrestrial base station (#1), and the base station and UAV (#2).

The approach consists of considering a software tool (ProMan-AWETM) that facilitates to compare the signal prediction between different propagation models while adjusting several parameters from the model to fit it, as close as possible, to the characteristics of the real scenario.

The remaining of the paper is organized as follows. Section II describes several terrestrial communications propagation scenarios and existing models. Section III presents measurement results for terrestrial communications with UAVs obtained during the field trials. Section IV proposes the new empirical propagation model for UAVs. Finally, Section V draws the conclusions and presents suggestion for future work.

II. TERRESTRIAL PROPAGATION SCENARIO AND MODELS

The generalized Lisbon University Institute (LUI) propagation model is being developed to consider an outdoor scenario, with frequency bands from Global System for Mobile Communications (GSM) [1], Universal Mobile Telecommunication System (UMTS) [2] and Long Term Evolution (LTE) [3]. It considers that the receiver antenna at the hexacopter is moving in 3D coordinates. By studying the different mobile communication technologies, it has also been fundamental to consider Table I, which shows the different receiver sensitivities for the different mobile technologies and also provides some insight on the range for a communication or video transmission between the hexacopter and the antenna.

Different propagation models available in the literature include the ones that had some common characteristics with the model being developed (e.g., correspond to the same type of scenario). These models include the Friis, Okumura, COST - 231 Hata, COST Walfisch-Ikegami, Ericsson 9999, SUI and LUI models [4], [5], [6]. After analyzing such models, it is possible to identify some differences between them. The limitations are due to the fact that each of them was developed for a specific scenario, with one or more technologies.

Some of the most important parameters are the frequency (as shown in Fig. 2), base station height and receiver antenna height. It is worthwhile to understand the limitations from each model arising from each of these parameters. An example of the performed study and frequency range covered by each model follows.

TABLE I. - RECEIVER SENSITIVITY FOR DIFFERENT TECHNOLOGIES

Technology	Receiver sensitivity [dBm]
GSM 900/1800 speech	-110
UMTS speech	-125
UMTS (64 kbps)	-120
UMTS (144 kbps)	-117
UMTS (384 kbps)	-113
LTE (1024 kbps)	-106

III. FIELD TRIALS AND MEASUREMENTS

The WinPropTM network planning tool from AWE Communications [7] has been considered for simulation purposes, more specifically a tool called ProMan, which can simulate signal propagation in certain environments. Figure 3 presents an example of results obtained with ProMan with an antenna with 10 degree tilt and base station height 15 m.

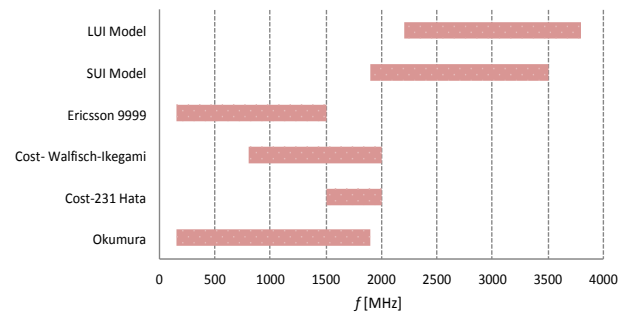


Fig. 2. - Propagation models versus frequency range.

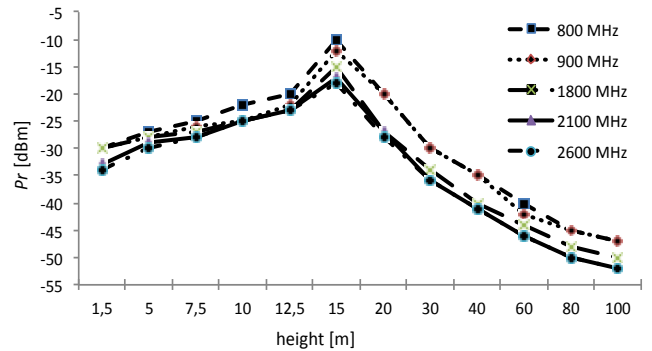


Fig. 3. - Simulated received power vs height, 10 degrees tilt.

Figure 4 shows the behaviour of the signal at a fixed height, varying in distance and also simulated for LTE using ProMan. And it can be observed that near the base station we have a value for the power and as we go a few meters apart from the centre we have better values for the received power. However, after a while (in this view graph around 30 meters) the values form the received power go down, because of the free space attenuation, which is higher as the mobile goes away from the base station.

To be able to measure the received power above an antenna, field trials consisted in using metrological balloons to lift a spectrum analyzer in the air with an antenna, alongside a laptop and a global positioning system (GPS). This experience allowed recording the received power that is being received by the aerial antenna connected to the spectrum analyzer while saving these results in the laptop through an interface software. Figure 5 shows the setup used during the experience and the balloons in the air with the LTE equipment.

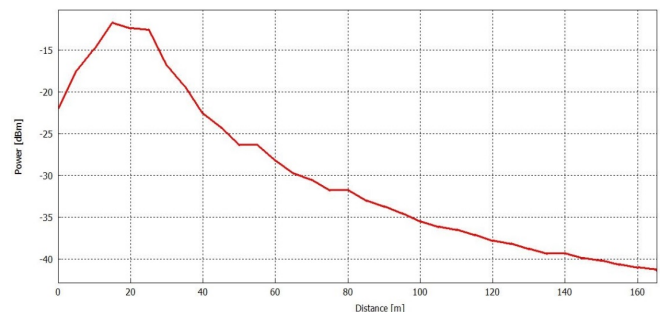


Fig. 4. - Simulated received power (P_r) versus distance, for a balloon at 10 meters height.



Fig. 5. – Balloons with equipment in the air to obtain experimental results.

Measurements have been done in four locations, to try and get enough knowledge on how the propagation signal goes from the ground to positions at high altitude. Figure 6 shows the set of results that have been obtained from experimental work with LTE for a distance from the origin in the xy plan of 8 m, where different colours for the curves identify different ranges for the height.

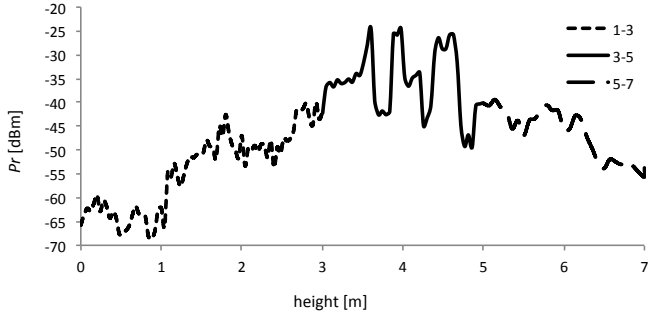


Fig. 6. - Received power vs height, for a distance from the origin in the xy plan of 8 m and 1800 MHz.

Figure 7 shows that there is a decreasing trend for height in the range 5-7 m and all three frequency bands, which corresponds to the received power decrease as altitude raises.

IV. LESSONS LEARNT AND PROPOSED MODEL

To develop the model, first it was fundamental to analyze the previous studied models, and identify a behaviour similar to the one from the results obtained with the experience and simulations. These values, obtained by testing the already existing propagation models with some specific values, are also important in the development of the propagation model. They can be considered for comparison purposes and serve as basis to the establishment of the propagation model.

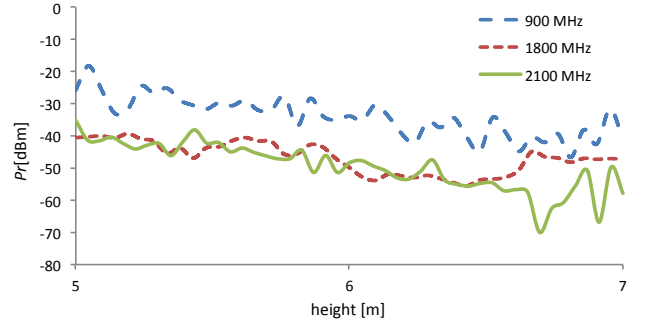


Fig. 7. – Received power as a function of the height (between 5 and 7 meters) for all frequency bands.

In the results from Fig. 8 some common parameters have been considered for all the models, similarly to the real scenario, but for only one frequency (1900 MHz). The proposed model has some unique characteristics: it is going to be for outdoor environment, operates within a frequency range from 800 to 2600 MHz, and heights of the terminal station and base station do not have limits. It also considers that the terminal station is going to move in 3D coordinates, as shown in Fig. 9, where θ is the elevation angle and Ψ is the tilt of the antenna. Figure 10 defines ϕ , which is the azimuth; β is the angle that determines if the antenna is sectorial ($\beta \neq 0$ and $\beta \neq 360$ degrees).

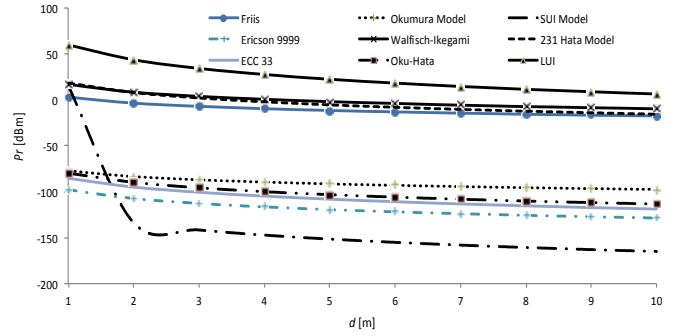


Fig. 8. - Existing propagation models.

As such, knowing all the options for the development of the model, the propagation model developed is described by (1), where the Path Loss (PL) is the average attenuation between the transmitter and receiver, in dB.

$$PL(d) = 20 \cdot \log\left(\frac{4\pi d_0}{\lambda}\right) + X_d + X_f + X_{ang} + X_{hei} \quad (1)$$

where

$$X_d = 10 \cdot \gamma_1 \cdot \log\left(\frac{d}{d_0}\right) \cdot \mathbf{u}(d_{bp} - d), \quad (2)$$

$$X_{ang} = \mathbf{u}(h_{TS} - h_{BS}) \cdot X_{angles}, \quad (3)$$

and

$$X_{hei} = [\mathbf{u}(h_{TS}) - \mathbf{u}(h_{TS} - h_{BS})] \cdot X_h \quad (4)$$

This first part of (1) is equal to LUI Model equation for outdoor environments, as shown in [8]. It is also the equation used when considering only 2D coordinates. If 3D coordinates are considered, d is now in fact $d(x, y, z)$, as shown in (5). It also has a new correction factor X_{angles} .

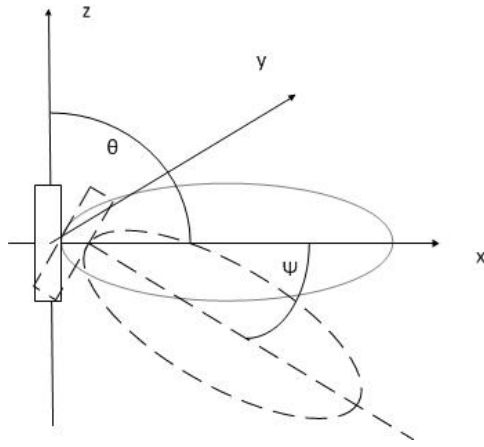


Fig. 9. - Coordinate system for the propagation model elevation and tilt.

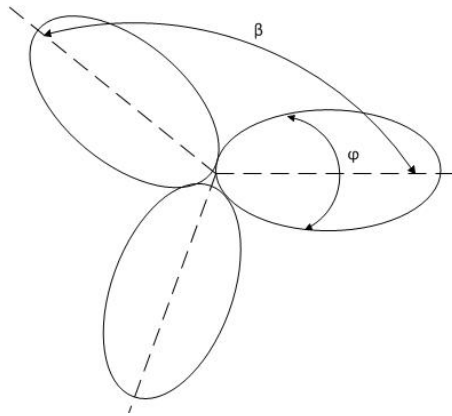


Fig. 10. - Coordinate system for the propagation model azimuth and sectorization.

It also has a new correction factor X_{angles} .

$$d = \sqrt{(x_1 - x_2)^2 + (y_1 - y_2)^2 + (z_1 - z_2)^2} \quad (5)$$

d_0 represents the reference distance which is determined from measurements, done close to the transmitter, different reference distance lead to different path loss exponents. In the case of this paper the measures have been performed few meters away from the base station. So, the size of $d_0 = 1\text{m}$ was considered in this work.

X_f and X_h are the correction factors for the frequency and base station height, the respective equations are according to [8], [9]. Also X_h is being multiplied by $[u(h_{TS}) - u(h_{TS} - h_{BS})]$ because this correction factor is only for heights between 2 and 10 meters for the terminal station height (h_{TS}).

γ_1 or path loss exponent equation has also been modified, and is now as shown in (6). The objective was that while the terminal station is below the base station antenna height it works as before as LUI Model for lower altitudes, but at higher altitudes it gets a new value. h_b is considered to be between 0 and 200 meters, a , b and c are values that come from the table 3.2 of LUI model and vary according to the environment, urban, suburban and rural.

$$\gamma_1 = \left[a - b \cdot h_b + \left(\frac{c}{h_b} \right) \right] \cdot \xi_1 + \xi_2 \quad (6)$$

where

$$\xi_1 = [u(h_{TS}) - u(h_{TS} - h_{BS})] \quad (7)$$

and

$$\xi_2 = 2 \cdot u(h_{TS} - h_{BS}) \quad (8)$$

where $u(h_{TS} - h_{BS})$ is a unit step function of discrete values, and according to the result (0 or 1) the adjacent parameters that are being multiplied by these functions are null or not. Equation (9) represents this function:

$$u(h_{TS} - h_{BS}) = \begin{cases} 0, & \text{if } h_{TS} < h_{BS} \\ 1, & \text{if } h_{TS} \geq h_{BS} \end{cases} \quad (9)$$

and $[u(h_{TS}) - u(h_{TS} - h_{BS})]$ is a rectangular function. It is similar to the unit step function, with the same result (0 or 1) but in this function only along a specific interval, as it can be obtained by equation (10):

$$[u(h_{TS}) - u(h_{TS} - h_{BS})] = \begin{cases} 0, & 0 \leq h_{TS} \\ 1, & 0 < h_{TS} < h_{BS} \\ 0, & h_{TS} \geq h_{BS} \end{cases} \quad (10)$$

X_{angles} is the correction factor for the different angles, and its value is the minimum value between $X_{\theta+\psi}$ and $X_{\varphi+\beta}$ which are the correction factors for elevation and azimuth respectively:

$$X_{\text{angles}} = \min(X_{\theta+\psi}, X_{\varphi+\beta}) \quad (11)$$

This factor is multiplied by $u(h_{TS} - h_{BS})$, because below the base station antenna height the previous LUI model already had good results and without this term the attenuation below the base station would be higher than it is supposed to be.

$X_{\theta+\psi}$ is the correction factor for the elevation as described previously, it also takes in account the tilt as can be observed in equation (12):

$$X_{\theta+\psi} = [1 - \delta(\theta + \Psi)] \cdot F \quad (12)$$

where

$$F = [0.0031(\theta + \Psi)^2 - 0.6511(\theta + \Psi) - 4.447] \quad (13)$$

To understand the representation of the tilt and elevation one observes Fig. 9, where θ and Ψ represent the elevation and tilt of the antenna respectively. The elevation (θ) is calculated according to the rules of trigonometry, as described in (14), where the distance is going to depend on x and y values. The tilt (Ψ) is limited by the antenna specifications, but its value is usually between 0 and 15 degrees.

$$\|\tan(\theta)\| = \frac{\text{terminal height} - \text{base station height}}{\text{distance}(x,y)} \quad (14)$$

$X_{\varphi+\beta}$ is the correction factor for azimuth, that also takes in account β . Equation (15) is used for this correction factor.

$$X_{\varphi+\beta} = [1 - \delta(\varphi + \beta)] \cdot (-0.0018) \cdot (\varphi + \beta)^2 - G \quad (15)$$

where

$$G = 0.0377 \cdot (\varphi + \beta) - 0.2115 \quad (16)$$

Also, by observing Fig. 10, it is possible to understand better what are the azimuth and β . This β is a variable that represents which sectorization is being used. $\delta(\theta + \Psi)$ is a Dirac delta function.

By analyzing the simulated results, first it can be concluded that with a larger down tilt the received power is higher for lower heights, and it starts to decrease till some point. After 30 meters it seems to be very similar to every down tilt that was simulated. When the receiver reaches higher altitudes, from all the results obtained we can see that the lowest frequency bands correspond to the highest receiver power, and it seems that till the altitude of 30 meters all the frequency bands have a very similar behaviour in all the view graphs.

In the view graph from Fig. 11 one can observe the occurrence of the gap that was expected to happen with the obtained simulation results from Fig. 4. This example is for the case where the hexacopter is at 19 meter height. When it is over the base station the received power significantly decreases mostly due to the null from the antenna pattern. However, as the hexacopter moves along distance (x, y) the received power first starts to enhance, again because of the antenna pattern and the lowest path loss. However, after some distance (around 14 meters in this view graph) the received power starts to decrease again. This can be explained because the path loss starts to increase and the gain due to the antenna pattern is not high enough to counteract this effect. Hence, the received power will continue to decrease constantly with the distance. Also if we compare the positive half (distance axis) of this view graph with the modelling results for LTE from Fig. 12 the behaviour is very similar, even though the heights are different. By observing graphic from Fig. 12, the received power curve decreases as height of the terminal station rises, and also fixed at a distance of 8 meters from the origin of the xy plan and base station height of 15 meters.

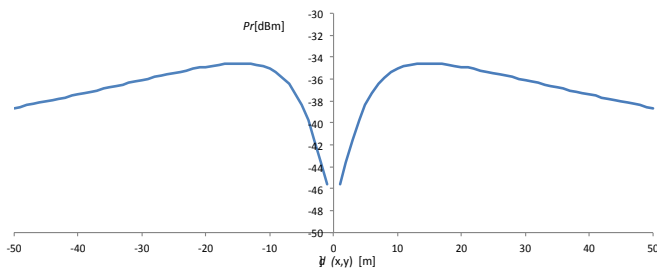


Fig. 11. - Gap above base station antenna, at 19 meters height (results are obtained through the use of the proposed model).

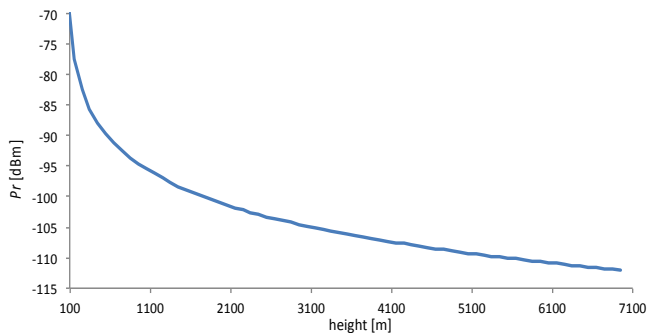


Fig. 12. - Threshold for communications as a function of height.

It can be concluded that to guarantee high quality video, the hexacopter can fly to heights of around 3.5 km.

Fig. 13 now shows the received power as a function of the distance (instead of the receiver terminal height) for a height of 19 m. In several references and specifications on LTE it is mentioned that “LTE deliver optimum performance in a cell size of up to 5 km. It is still capable of delivering effective performance in a cell size of up to 30 km”. This can be true since the effective cell size depends on an equation which also depends on many factors, as it can be seen in [10]. So, having this in mind, it is possible to conclude from Fig. 13 that there will not be limitations as long as the hexacopter or another terminal station is around the 5 km distance from the base station, or even more, depending on some other parameters.

V. CONCLUSION AND FUTURE WORK

In this work we have assessed the performance of terrestrial cellular networks regarding the control and monitoring of UAVs. Our main contribution is a new propagation model, based on experiments in one scenario of interest and subsequent analysis of the measured data. The model was obtained with the GSM, UMTS and LTE technologies in mind and can be included in current cellular wireless planning tools to perform 3D planning.

We have concluded that the worst case scenario corresponds to the situation when the UAV flies over the base station. It is found that the received power is minimum for this scenario due to the radiation pattern of the antenna. We note, however, that in this situation the UAVs can do handover for adjacent base stations. Therefore, more experimental work is necessary to measure several delays for handover, depending on the UAVs velocity.

Left for future studies is the improvement of the propagation model in different scenarios. For example, another measurement campaign is planned near the cell edges to characterize the behaviour of the hexacopter regarding base station switching. On a handover, the possibility that the hexacopter loses the connection with the ground operator (the person controlling the UAV), with the possibility of stopping the broadcast of real-time video, is a real possibility.

Our results can also be complemented with other type of measurement campaigns, since our study was focused in a specific scenario and we want to transform the LUI model to a more general propagation model.

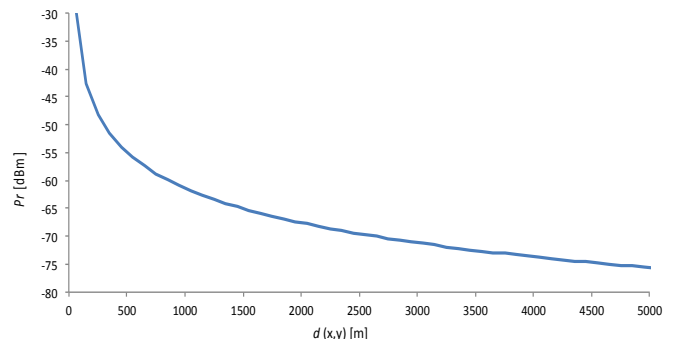


Fig. 13. - Threshold for communications as a function of d , 19 m height.

ACKNOWLEDGMENT

The authors acknowledges to SAAS, CREaTION and UID/EEA/50008/2013.

REFERENCES

- [1] <http://www.3gpp.org/technologies/keywords-acronyms/102-gprs-edge> (accessed on April of 2014).
- [2] <http://www.3gpp.org/technologies/keywords-acronyms/103-umts> (accessed on April of 2014).
- [3] F. Kow, C. Chiang, H. Hsu, T. Huang, and R. Sung, "A New Approach for Radiation Pattern Measurement of RFID Tag Antenna Under Chip-loaded Condition Using Friis Equation", in *Proc. of Asia-Pacific Microwave Conference 2010*.
- [4] <http://www.3gpp.org/technologies/keywords-acronyms/98-lte> (accessed on April of 2014).
- [5] N. Shabbir, T. Muhammad, K. Hasnain, and U. Rizwan, "Comparison of Radio Propagation Models for Long Term Evolution (LTE) Network", *International Journal of Next-Generation Networks*, Volume 3.
- [6] T. Rappaport, "Wireless Communications: Principles and Practice", 2nd edition, Prentice Hall, 2002.
- [7] <http://www.awe-communications.com/Products/index.html> (accessed on April of 2014).
- [8] F. Varela, P. Sebastião, A. Correia, F. Cercas, A. Rodrigues, F. Velez, and D. Robalo, "Unified propagation model for Wi-Fi, UMTS and WiMax planning in mixed scenarios", in *Proc. of IEEE 21st International Symposium on Personal Indoor and Mobile Radio Communications (PIMRC)*, pp. 81-86, Instambul, 26-30, Sept. 2010.
- [9] F. Varela, P. Sebastião, A. Correia, F. Cercas, A. Rodrigues, F. Velez, and D. Robalo., "Validation of the unified propagation model for Wi-Fi, UMTS and WiMax planning", *IEEE 21st International Symposium on Personal Indoor and Mobile Radio Communications (PIMRC)*, pp. 87-92, Instambul, 26-30, Sept. 2010.
- [10] W. Afric, S. Pilinsky, "UMTS LTE Downlink Cell Size Calculation", *54th International Symposium ELMAR-2012*, pp. 12-14, 2012.